HHS Public Access

Author manuscript

Sci Transl Med. Author manuscript; available in PMC 2016 February 24.

Published in final edited form as:

Sci Transl Med. 2015 March 18; 7(279): 279ra41. doi:10.1126/scitranslmed.aaa4691.

Improved antitumor activity of immunotherapy with BRAF and MEK inhibitors in BRAF^{V600E} melanoma

Siwen Hu-Lieskovan[1], **Stephen Mok**[1], **Blanca Homet Moreno**[1,2], **Jennifer Tsoi**[3], **Lidia Robert Faja**[1], **Lucas Goedert**[1], **Elaine M. Pinheiro**[4], **Richard C. Koya**[1,**], **Thomas Graeber**[3,6,7], **Begoña Comin-Anduix**[5,6], and **Antoni Ribas**[1,5,6,7,*]

[1]Department of Medicine, Division of Hematology-Oncology, University of California Los Angeles, Los Angeles, California (UCLA).

[2]Division of Translational Oncology, Carlos III Health Institute, Madrid, Spain.

[3]Crump Institute for Molecular Imaging, UCLA.

[4]Merck Research Laboratories, Boston, MA

[5]Department of Surgery, Division of Surgical-Oncology, UCLA.

[6]Department of Molecular and Medical Pharmacology, UCLA.

[7]Jonsson Comprehensive Cancer Center at UCLA.

Abstract

Combining immunotherapy and BRAF targeted therapy may result in improved antitumor activity with the high response rates of targeted therapy and the durability of responses with immunotherapy. However, the first clinical trial testing the combination of the BRAF inhibitor vemurafenib and the CTLA-4 antibody ipilimumab was terminated early due to substantial liver toxicities. MEK inhibitors can potentiate the MAPK inhibition in BRAF mutant cells, while potentially alleviating the unwanted paradoxical MAPK activation in BRAF wild type cells that lead to side effects when using BRAF inhibitors alone. However, there is the concern of MEK inhibitors being detrimental to T cell functionality. Using a mouse model of syngeneic *BRAF*^{V600E} driven melanoma, we tested whether addition of the MEK inhibitor trametinib would enhance the antitumor activity of combined immunotherapy with the BRAF inhibitor dabrafenib. Combination of dabrafenib and trametinib with pmel-1 adoptive cell transfer (ACT) showed complete tumor regression, increased T cell infiltration into tumors and improved *in vivo* cytotoxicity. Single agent dabrafenib increased tumor-associated macrophages and T regulatory cells (Tregs) in tumors,

[*]**Correspondence:**Antoni Ribas, M.D, Ph.D., Department of Medicine, Division of Hematology-Oncology, 11-934 Factor Building, Jonsson Comprehensive Cancer Center at UCLA, 10833 Le Conte Avenue, Los Angeles, CA 90095-1782, USA. Telephone: 310-206-3928. Fax: 310-825-2493. aribas@mednet.ucla.edu..

[**]Author current address: Department of Immunology, Roswell Park Cancer Institute, Buffalo, New York

Author contributions: S.H-L., S.M., B.H.M., L.R., L.G., E.M.P., R.C.K. and B.C-A. performed the experiments. J.T. and T.G. analyzed the gene expression profiling. S.H-L. and A.R. designed the experiments and wrote the manuscript.

Competing interests: The authors declare no conflicts of interest.

Data and materials availability: Dabrafenib and trametinib were obtained through an MTA with GSK. DX400 murine PD-1 antibody was obtained through an MTA with Merck. The gene expression profiling is available at http://www.ncbi.nlm.nih.gov/geo/info/submission.html (Accession number: GSE64102).

which decreased with the addition of trametinib. The triple combination therapy resulted in increased melanosomal antigen and MHC expression, and global immune-related gene up-regulation. Given the up-regulation of PD-L1 seen with dabrafenib and/or trametinib combined with antigen-specific ACT, we tested combination of dabrafenib, trametinib with anti-PD1 therapy in SM1 tumors, and observed superior anti-tumor effect. Our findings support the testing of triple combination therapy of BRAF and MEK inhibitors with immunotherapy in patients with $BRAF^{V600E}$ mutant metastatic melanoma.

Introduction

The recent breakthroughs brought by the clinical use of immune checkpoint inhibition in cancer provide an exciting promise of long-term responses in clinically significant numbers of patients (1-5). Strategies to extend this low frequency event to the majority of patients have become the focus of cancer immunotherapy research. In BRAF mutant melanoma, the combination of BRAF inhibitors and immunotherapy has been tested in both preclinical models and clinical trials (6-9). This is based on the targeting of the $BRAF^{V600E}$ driver mutation, present in approximately 50% of metastatic melanomas, and the immunosensitization effects of BRAF inhibitors through increased antigen presentation (10-12), antigen-specific T cell recognition(10, 13), homing of immune effector cell to the tumors (12, 14, 15) and improved T cell effector functions(6, 16). However, the benefit of this combination in preclinical models has been modest (6-9), while substantial liver toxicity was observed in the first clinical trial combining the BRAF inhibitor vemurafenib and the CTLA4 blocking antibody ipilimumab (17). Both the improved effector function and the toxicities were attributed to the paradoxical activation of the MAPK pathway by vemurafenib in BRAF wild type cells (18).

MEK inhibitors, on the other hand, can potentiate the antitumor effects in the melanoma cells (19) and reduce toxicity associated with BRAF inhibitors (18), given their ability to inhibit MAPK signaling in cells with and without a BRAF mutation (20). In addition, MEK inhibitors have demonstrated potential of immunosensitization by up-regulation of tumor antigen expression and presentation (10, 21), serving as a rational addition to the BRAF inhibitor and immunotherapy combination. However, there is theoretical concern that a MEK inhibitor could dampen immune effector functions, given that *in vitro* studies have shown impaired T cell proliferation and functions with MEK inhibition (10, 22). Alternatively, when combining with BRAF inhibitors, MEK inhibitors might balance the potential overreacting effector cells to avoid exhaustion, and improve the tumor microenvironment by influencing the cytokine production and immune suppressive cell populations in the tumor microenvironment (20).

Using a syngeneic $BRAF^{V600E}$ mutant melanoma mouse model (6), we tested the hypothesis that the addition of a MEK inhibitor would enhance the immunosensitization effects of BRAF inhibition, with increased antitumor activity and decreased toxicity.

Results

Enhanced *in vivo* antitumor activity with pmel-1 adoptive cell transfer (ACT), dabrafenib and/or trametinib

We derived a $BRAF^{V600E}$ mutant murine melanoma SM1, syngeneic to fully immune-competent C57BL/6 mice, from a spontaneously arising melanoma in $BRAF^{V600E}$ transgenic mice (6). Besides the presence of the $BRAF^{V600E}$ transversion, SM1 also has CDKN2A gene deletion and BRAF and MITF gene amplification, and is only moderately sensitive to vemurafenib (6). In this study, we first confirmed the downstream MAPK pathway inhibition of SM1 after treatment with dabrafenib, trametinib, or the combination *in vitro* by down-regulated phosphorylated ERK (Fig. 1A). To further explore the drug effects on effector T cells, we treated $gp100_{25\text{-}33}$-activated pmel-1 mouse splenocytes with serial dilutions of dabrafenib, trametinib, or dabrafenib plus trametinib. Western blot analysis at 24 hours of treatment showed paradoxical activation of the MAPK pathway with dabrafenib alone at medium and high concentrations, evidenced by increased phosphor-ERK (Fig S1A). Trametinib alone or with dabrafenib blocked the MAPK pathway even at low doses. However, *in vitro* cell viability (MTS) assay with concentration up to dabrafenib 40μM, and trametinib 2μM did not show any decreased cell viability at 72 hours (Fig S1B).

We then tested the antitumor effects of dabrafenib, trametinib and the combination *in vivo* against established SM1 tumors in syngeneic mice. SM1 tumors established subcutaneously in C57BL/6 mice responded to combination therapy of dabrafenib and trametinib, with a statistically significant difference in growth inhibition when compared with tumors treated with dabrafenib or trametinib alone, or vehicle control (Fig. 1B, $p=0.002$, unpaired t test, $n=4$, mean+/−SD). We then tested the combinatorial effect of dabrafenib, trametinib and immunotherapy using the pmel-1 ACT model, which is based on T cells transgenic for a T cell receptor (TCR) recognizing the murine melanosomal antigen gp100 (23), endogenously expressed by SM1 (Fig. 1C). Myeloid-depleted C57BL/6 mice with bone marrow transplant and established subcutaneous SM1 tumors received ACT of $gp100_{25\text{-}33}$ peptide activated splenocytes obtained from pmel-1 mice. Wild type C57BL/6 mouse splenocytes activated non-specifically by CD3 and CD28 were administered as mock ACT controls. Both ACT were followed by three days of high dose IL-2 injections. In three replicate experiments, the triple combined therapy of dabrafenib, trametinib with pmel-1 ACT provided superior antitumor activity against established SM1 tumors with complete tumor regression, not observed with pmel-1 ACT plus either BRAF or MEK inhibitor therapy alone, or mock ACT with both dabrafenib and trametinib (Fig. 1D).

Increased effector T cell homing to the tumors associated with both dabrafenib and trametinib

To analyze the mechanism of improved antitumor activity with the triple combination therapy, we first evaluated the expansion and change in distribution of adoptively transferred cells *in vivo*. Tumors and spleens were harvested on day 5 after ACT and stained for CD3, CD8 and Thy1.1 (expressed by the pmel-1 mice but not the wild type C57BL/6 mice). There was statistically significant increase of CD3+Thy1.1+ (adoptively transferred pmel-1 effector) and CD3+CD8+ (both endogenous and adoptively transferred effector) cells in the

tumors treated with dabrafenib, with trametinib or with the combination of dabrafenib plus trametinib when compared to vehicle-treated mice (unpaired t test, n=3, mean+/−SD, Fig. 2A and 2B). On the other hand, effector cells harvested from the spleen did not show statistically significant difference in distribution between the treatment groups (Fig 2A). To analyze the effects on the whole animal, we genetically labeled the adoptively transferred cells with the firefly luciferase transgene to track these cells *in vivo* using bioluminescence imaging (Fig 2C, imaged 5 days after ACT). The quantitative analysis of luciferase activity over time in the living mice showed peaked tumor infiltrating effector T cell five days after ACT. SM1 tumors treated with triple combination therapy, pmel-1 ACT plus dabrafenib or pmel-1 plus trametinib, showed significantly higher accumulation of adoptively transferred effector cells than those tumors treated by pmel-1 ACT alone (Fig. 2D, unpaired t test, n=4, mean+/−SD).

No impaired effector function *in vivo* associated with trametinib

Given the concern that MEK inhibitors might impair effector T cell function (10), we evaluated the effect of dabrafenib and trametinib on T cell effector function both *in vitro* and *in vivo*. When $gp100_{25\text{-}33}$-activated pmel-1 mouse splenocytes were exposed *in vitro* to increasing concentrations of dabrafenib and trametinib for 72 hours, there was significant decrease of interferon gamma- producing effector cells associated with medium and high concentrations of both dabrafenib and trametinib (Fig. 3A, unpaired t test, n=3, mean+/−SD). To test the effects of the combination therapy *in vivo*, tumors and spleens were harvested 5 days after ACT and analyzed for the activation state of T cells. Adoptively transferred effectors T cells (CD3+Thy1.1+) collected from mice treated with pmel-1 ACT plus trametinib or triple combination therapy did not show statistically significant differences compared to pmel-1 plus vehicle control in the ability to respond to short-term *ex vivo* re-stimulation with the $gp100_{25\text{-}33}$ antigen assessed by IFN gamma secretion (Fig. 3B-3C, unpaired t test, n=3, mean+/−SD). We then tested the direct effect of dabrafenib and trametinib on lymphocyte cytotoxicity *in vivo* independent of their effects on SM1 tumor cells using an *in vivo* cytotoxicity assay, where the targets are syngeneic splenocytes devoid of the $BRAF^{V600E}$ mutation and pulsed with $gp100_{25\text{-}33}$ or control peptides (Fig 3D). Pmel-1 ACT induced potent cytotoxic effects against splenocytes pulsed with the $gp100_{25\text{-}33}$ peptide, but not against the control OVA peptide (34% lower $gp100_{25\text{-}33}$ target intensity, p=0.01 pmel-1 V vs mock V, unpaired t test, n=3, mean+/−SD). The cytotoxicity increased with systemic treatment of pmel-1 ACT plus dabrafenib, but this was not statistically significant (Fig. 3E-3F, Fig. S1D), and there was no difference in cytotoxic activity with pmel-1 plus trametinib and triple combination therapy when compared to pmel-1 ACT plus vehicle control. Therefore, the addition of trametinib to dabrafenib did not change the functionality of adoptively transferred pmel-1 cells in terms of their ability to release immune stimulating cytokines and intrinsic antigen-specific lytic activity *in vivo*.

Improved tumour microenvironment when trametinib was combined with dabrafenib and ACT

To evaluate the effect of dabrafenib, trametinib and the combination on other cellular components of the tumour microenvironment, we harvested spleens and tumours 5 days after ACT, and studied the cell populations by multiplex FACS. We first analyzed the

myeloid-derived suppressor cells (MDSC), a heterogeneous group of cells that induce tumor-associated immune suppression. MDSCs (Gr+CD11b+) were present at a low level in SM1 tumors (<5%) and their level increased with antigen-specific ACT (Fig. S1C). Pmel-1 ACT plus dabrafenib significantly increased MDSCs in the tumors when compared to pmel-1 ACT plus vehicle control group ($p=0.02$, unpaired t test, n=3, mean+/−SD), with a non-significant trend of decreased MDSCs in the spleen. Trametinib, or dabrafenib plus trametinib with pmel-1 ACT did not change MDSCs in the tumors or spleens when compared to pmel-1 ACT plus vehicle. MDSCs consist of two major subsets: cells with granulocytic phenotype that express Ly6G marker (PMN-MDSC, Ly6ClowLy6GhighCD11b+) and cells with monocytic phenotype expressing Ly6C marker (MO-MDSC, Ly6ChighLy6GlowCD11b+) (Fig. S1E). These two subsets of MDSCs have distinct functions in infection, autoimmune diseases and cancer (24). We examined these two subsets of MDSCs, presented as percentage of CD11b+ cells. As shown in Fig 4A and 4B, there was a significant shift of MDSC subsets in the tumours towards increased MO-MDSCs and decreased PMN-MDSCs, associated with both dabrafenib, trametinib and combination treatments. Whereas in the spleen, other than a decreased percentage of MO-MDSC with pmel-1 ACT plus dabrafenib treated mice vs pmel-1 ACT plus vehicle control ($p=0.06$, unpaired t test, n=3), there was no significant change among the different treatment groups. We then analysed mature tumour-associated macrophages (TAMs, F4/80+CD11b+). Both pmel-1 ACT plus dabrafenib and triple combination therapy significantly increased macrophages in the tumours (Fig 4C, 4E), but to a lesser extent with triple combination, while no change was seen with pmel-1 ACT plus trametinib. There was no significant change in macrophages in the spleen among the different treatment groups. Analysis of another immune suppressive cell population, the T regulatory cells (Tregs, CD4+CD25+FOXp3+) showed significantly increased percentage in the tumours with pmel-1 ACT plus dabrafenib treatment (Fig S1F, $P=0.002$, unpaired t test, n=3) but no other significant change with the other combination therapies in both tumor and spleen (Fig 4D, 4E). These results indicated that dabrafenib, when combined with pmel-1 ACT and IL-2, increases macrophage and Tregs infiltration in the tumor microenvironment, thus providing a potential mechanism for the suboptimal antitumor effect with this combination. This effect on macrophage and Tregs can be overcome by the addition of trametinib. Moreover, both dabrafenib and trametinib can shift the ratio of MDSC subsets from PMN-MDSC to predominantly MO-MDSC.

Increased immune-related gene expression by both dabrafenib and trametinib treatments

In order to better understand the impact of dabrafenib and trametinib on the tumor microenvironment, we compared the gene expression profiling of SM1 tumors by microarray analysis following 5-day treatment with dabrafenib, trametinib, or the combination with pmel-1 or mock ACT. Two to three replicates were prepared per treatment group after the samples had passed quality control by gel electrophoresis (Fig S2A). The expression level of each gene was averaged across samples and used for further analysis. As shown in Fig 5A by principal component analysis (PCA) and Fig S2B by hierarchical clustering of global gene expression, the biological replicates cluster together closely and separate from each other according to the different treatments. Clustering of immune related genes obtained from the gene ontology consortium under the GO term of immune system

process (http://www.geneontology.org; GO:0002376) showed three different patterns of gene expression changes (Fig 5B). Cluster A are genes up-regulated after treatment with dabrafenib, trametinib or the combination in mice receiving either mock ACT or pmel-1 ACT, and included melanoma antigens and many MAPK pathway genes. Also among them are CD274 (PD-L1) and CSF-1R. Cluster B are genes up-regulated by dabrafenib, trametinib or the combination when combined with antigen-specific pmel-1 ACT only, but not with the mock ACT. Many of these genes are MHC molecules, cytokines and chemokines or their receptors (Table S2). CD8, granzyme B and interferon gamma are within this group. Interestingly, CD83, a dendritic cell maturation marker (25), CD86, a ligand expressed on antigen-presenting cells that binds to CD28 and CTLA-4 (26), and CSF-1, are all in this gene cluster. Finally, cluster C are genes down-regulated by dabrafenib, trametinib or the combination in mice that received either mock ACT or pmel-1 ACT. Again this cluster included many MAPK pathway genes, as well as VEGF, a previously reported target of BRAF and MEK inhibition (27, 28). Another interesting gene in this cluster is CD276 (B7-H3), which was reported recently to be associated with advanced stage of melanoma progression (29). Further clustering of samples according to chemokines and their receptors showed a general trend of increased expression of these genes in the dabrafenib, trametinib or combination treated tumours, especially with triple combination therapy (Fig 5C). Expression of some genes previously reported to be regulated by BRAF inhibitors or mentioned above are shown in Fig S2C.

Increased tumor antigen and MHC expression in tumors treated by triple combination

One mechanism that tumors can evade the immune attack is via decreased tumor antigen or MHC expression. Analysis of the microarray data showed that both melanoma antigen and MHC expression are low in mock ACT plus vehicle and pmel-1 ACT plus vehicle (Fig 5D). Dabrafenib and trametinib significantly increased melanoma antigen expression in both pmel-1 ACT and mock ACT treated tumors, with the highest expression seen after triple combination treatment. However, the up-regulation of MHC molecules was restricted to the antigen-specific pmel-1 ACT-treated tumors with dabrafenib or/and trametinib, but not with mock ACT plus dabrafenib and trametinib, indicating that tumor-specific effector cells are important in the mechanism of MHC up-regulation.

Up-regulation of PD-L1 and enhanced *in vivo* antitumor activity with dabrafenib and/or trametinib with PD-1 blockade

Activated T cells express PD-1, which can bind to PD-L1 ligand up-regulated on tumor cells, and inhibit T cell effector functions. Recently, PD-1 and PD-L1 were found to be increased in melanoma tumor samples from patients treated with BRAF inhibitors (12), and addition of a MEK inhibitor suppressed the production of PD-L1 by *in vitro* study of melanoma cell lines (30). The up-regulation of IFN gamma, granzyme B expression and PD-1 in cluster B indicated increased effector T cell activation and function with dabrafenib and trametinib (Fig 6A). However, the up-regulation of PD-L1 suggested an adaptive immune resistance mechanism induced by the presence of effector T cells (Fig 6A). Flow cytometry analysis of PD-L1 expression of SM1 tumors after 5 days of treatment was consistent with the microarray gene expression data (Fig 6B), whereas no significant change was observed in the spleen samples. To test whether the increased IFN gamma in the tumor

milieu is sufficient for the up-regulation of PD-L1, we treated SM1 cells with increasing concentrations of IFN gamma and harvested cells for flow cytometry after 18 hours. The result showed that 1μg/ml of IFN gamma up-regulated PD-L1 on the surface of SM1 cells by more than 10 folds, similar to the B16 positive control cells (Fig 6C). This up-regulation of PD-L1 provided a rational for the combination of PD-1 blockade therapy with dabrafenib and trametinib. Immune-competent C57BL/6 mice with established subcutaneous SM1 tumors received PD-1 antibody or isotope control 200μg intraperitoneal injections every 5 days, started when the tumors reached 4-6 mm^2. Consistent with previous report (8), SM1 is innately resistant to PD-1 antibody therapy alone. In three replicate experiments, the combined therapy of dabrafenib, trametinib, and anti-PD1 provided superior antitumor activity against established SM1 tumors compared with anti-PD1 plus either therapy alone, or isotope control with both dabrafenib and trametinib (Fig. 6D).

Discussion

It has been previously reported that MEK inhibitors might be detrimental to T cell responses to cancer based mainly on *in vitro* studies (10, 22). However, by using an immune competent mouse model of $BRAF^{V600E}$ mutant melanoma, we demonstrate that the addition of the MEK inhibitor trametinib significantly improves the antitumor effect of the BRAF inhibitor dabrafenib and two modes of immunotherapy, ACT and PD-1 blockade, via improved effector T cell homing to the tumors, preserved effector function, increased tumor antigen and MHC expression, cytokine release, and attenuated immune suppressive cells up-regulated by the BRAF inhibitor in the tumor microenvironment.

Increased numbers of TILs have been reported in biopsies of patients treated with BRAF inhibitors (12, 14, 15), with an increase in clonality after BRAF inhibition and a better response in those patients who had a high proportion of pre-existing dominant TCR clones (31), suggesting that the T cell infiltration may be an antigen-driven recruitment into regressing tumors. In a xenograft model where a BRAF-mutant human melanoma cell line was transduced with gp100 and H-2D to allow recognition by gp100-specific pmel-1 mouse T cells, treatment with the BRAF inhibitor vemurafenib significantly increased the tumor infiltration and enhanced the antitumor activity of adoptively transferred T cells *in vivo* (27). This increased TIL infiltration was thought to be primarily mediated by decreased VEGF production by tumors via C-myc. Analysis of human melanoma biopsies before and during BRAF inhibitor treatment confirmed down-regulation of VEGF. Another syngeneic BRAF mutant melanoma model with $PTEN^{-/-}$ background tested the combination of vemurafenib and PD-1 and/or CTLA-4 blockade (9), and showed significantly increased T cell infiltration with vemurafenib alone. On the contrary, in an inducible BRAF mutant melanoma model there was decreased TIL after BRAF inhibition (7). In our SM1 model, previous study combining vemurafenib and pmel-1 ACT did not show increased TIL infiltration but did show improved effector function, likely through paradoxical activation of the MAPK pathway in T cells by vemurafenib (6, 16). With dabrafenib, titrated to higher concentrations to optimize antitumor activity, we observed both increased tumor T cell infiltration and improved functions. This is possibly due the different potency and concentration of the two BRAF inhibitors (we had used a lower dose with vemurafenib) [6]. Interestingly, we also observed decreased VEGF expression by microarray in the tumors treated with dabrafenib.

Trametinib increased the T cell homing to tumors, evidenced by *in vivo* imaging, *ex vivo* single tumor cell phenotyping, and microarray analysis. Evaluation of *in vivo* effector cell function by both cytokine releasing capacity and cytotoxic activity *in vivo* showed preserved effector functions after treatment with single agent trametinib, or dabrafenib plus trametinib.

One of the suggested mechanisms by which BRAF inhibitors may sensitize tumor to the immune system is via up-regulation of melanocyte differentiation antigens (MDA) and MHC expression in BRAF mutant melanoma (10-12). MEK inhibitors, on the other hand, can increase MDA expression in both BRAF mutant and wild type melanoma cells (10, 21). This should result in improved antigen-specific T-cell recognition (10, 13). Interestingly, it has been shown that MDA expression was significantly decreased in patients at the time of progression on BRAF inhibitors and restored when subsequent combined BRAF and MEK inhibitors were given (12). Consistent with the previous reports, our data suggest increased MDA and MHC expression in tumors treated by the combination therapy. Interestingly, the up-regulation of MDA is a drug effect, also seen in dabrafenib and trametinib combination with mock ACT. On the other hand, up-regulation of MHC is specific to the combination of dabrafenib, or trametinib, or dabrafenib plus trametinib with pmel-1 but not with mock ACT, indicating that antigen-specific effector activation is crucial for this regulation. Analysis of immune-related genes in the microarray data indicated other genes that are regulated in similar fashion: up- or down-regulated by drugs in both pmel-1 and mock ACT, or up-regulated by drugs in antigen specific ACT only. Clustering of chemokines and their receptors showed overall increased expression of many of these genes in tumors treated with the triple combination.

Despite the theoretical promise of increased tumor infiltrating T cells with improved function, increased tumor MDA and MHC expression, the combination of dabrafenib and pmel-1 ACT had only modest antitumor effects, with a small but statistically significant difference from mock ACT and pmel-1 ACT with vehicle control. This raised the possibility that the immune suppressive cells (MDSCs, TAMs, and Tregs) in the tumor microenvironment might inhibit effector T cell function. One of the main factors that negatively regulate the immune system are MDSCs, a heterogeneous population of immature myeloid cells (CD11b+Gr-1+ in mice) that are significantly expanded in patients with cancer and have been shown to correlate negatively with prognosis and overall survival (32). MDSCs have been shown to not only suppress immune responses, but also promote tumor growth and expansion in different tumor types (33-37). We observed an interesting shift of MDSC subtypes in the SM1 tumors, from PMN-MDSC subset to the MONO-MDSC subset, associated with both dabrafenib and trametinib, or combination treatment. This was correlated with significantly up-regulated tumor associated macrophages (TAMs, F4/80+CD11b+) and Tregs (CD4+CD25+FoxP3+) after treatment with dabrafenib combined with pmel-1 ACT, suggesting a potential immune evasion pathway. Microarray data showed concurrent up-regulation of CSF-1, CSF-1R, and the dendritic cell maturation marker CD83. Trametinib, however, did not increase TAM or Tregs when combined with pmel-1 ACT, and further attenuated the effect by dabrafenib when combined with both dabrafenib and pmel-1 ACT. This might have accounted for the significantly different antitumor effects of triple combination therapy compared to dabrafenib plus pmel-1 ACT.

PD-1 expression is induced on activated T cells, which in turn binds to its ligand PD-L1 and negatively regulates TCR signaling (38-40). Increased T cell exhaustion markers, including TIM3, PD-1 and PD-L1, were noted in tumor samples from patients treated with BRAF inhibitors suggesting a potential resistance mechanism (12). One *in vitro* study of melanoma cell lines showed increased PD-L1 expression by BRAF inhibitor-resistant melanoma cells, mediated by c-JUN and STAT3 signaling, and addition of a MEK inhibitor suppressed the expression of PD-L1 (30). Our study showed improved effector activity manifested by increased IFN gamma and granzyme B expression, which coincides with the up-regulation of PD-1 and PD-L1, unique to the tumor milieu. We also showed that IFN gamma is sufficient for the up-regulation of PDL1 on SM1, consistent with published reports (39), which also explained why MEK inhibitor-treated tumors also had elevated PD-L1 expression, and again stressed the importance of the *in vivo* environment to study immune responses. Given that CD8 T cells are the effectors of PD-1 blockade, and the up-regulation of PD-L1 seen with both dabrafenib and trametinib treatments when combined with antigen specific ACT, we tested the triple combination of dabrafenib, trametinib and anti-PD1 therapy, and observed significant synergy of this combination to inhibit SM1 tumor growth. This anti-tumor activity was most significant with the triple therapy, but was also notable for the combination of either dabrafenib or trametinib plus anti- PD1 therapies.

Our results are limited to preclinical models and need to be validated in clinical trials. Several phase I clinical trials are ongoing combining BRAF and MEK inhibitors with immunotherapies such as anti-CTLA4, anti-PD-1, anti-PD-L1 and ACT (20), and our data suggests that the presence of a MEK inhibitor will improve the effects of the combined therapy as opposed to the concern of limiting T cell responses to cancer.

Materials and Methods

Study design

The primary research objective was to evaluate combinatorial strategies of BRAF inhibitor, MEK inhibitor and adoptive cell transfer or PD-1 blockade. The overall study design was a series of controlled laboratory experiments in mice, as described in the sections below. In all experiments, animals were assigned to various experimental groups in random. The experiments were replicated two to three times as noted. For the experiments reporting isolation of TILs, three mice per group were used for each experiment, with two to three replicates. All outliers were included in the data analysis.

Mice, cell lines, and reagents

C57BL/6 mice (Thy1.2, Jackson Laboratories) and pmel-1 (Thy1.1) transgenic mice were bred and kept under defined-flora pathogen-free conditions at the Association for the Assessment & Accreditation of Laboratory Animal Care-approved animal facility of the Division of Experimental Radiation Oncology, UCLA, and used under the UCLA Animal Research Committee protocol #2004-159. The SM1 murine melanoma was generated from a spontaneously arising tumor in $BRAF^{V600E}$ mutant transgenic mice as previously described(6). The tumor was minced and implanted into C57BL/6 mice for *in vivo* experiments. Part of the minced tumor was plated under tissue culture conditions as SM1

cell line, maintained in RPMI (Mediatech) with 10% fetal calf serum (Omega Scientific), 2 mmol/L L-glutamine (Invitrogen), and 1% (v/v) penicillin, streptomycin, and amphotericin (Omega Scientific). Dabrafenib and trametinib were obtained under a materials transfer agreement with GSK. Dabrafenib and trametinib were dissolved in dimethylsulfoxide (DMSO; Fisher Scientific) and used for in vitro studies. For in vivo studies, dabrafenib and trametinib were suspended in an aqueous mixture of 0.5% hydroxypropyl methyl cellulose (HPMC) and 0.2% tween 80 (Sigma-Aldrich). One hundred μL of the suspended drug was administered by daily oral gavage into mice at 30 mg/kg of dabrafenib or/and 0.6mg/kg of trametinib when tumors reached 5 mm in diameter. Mouse PD-1 antibody (DX400) was obtained under a materials transfer agreement with Merck.

Cell viability assays

SM1 cells, naive C57BL/6 splenocytes, or activated pmel-1 splenocytes were seeded in 96-well flat-bottom plates (5000 cells/well) with 100 mL of 10% fetal calf serum media and incubated for 24 hours. Serial dilutions of dabrafenib, trametinib or DMSO vehicle control, in culture medium, were added to each well in triplicate and analyzed following the MTS assay (Promega).

Western blotting

Cells were washed with ice-cold PBS before lysed using a lysis buffer containing 10 mmol/L Tris, pH 7.4, 100 mmol/L NaCl, 1 mmol/L EDTA, 1 mmol/L EGTA, 1 mmol/L NaF, 20 mmol/L $Na_4P_2O_7$, 2 mmol/L Na_3VO_4, 0.1% sodium dodecyl sulfate, 0.5% sodium deoxycholate, 1% Triton X-100, 10% glycerol, 10 μg/mL leupeptin, 60 μg/mL aprotinin, and 1 mmol/L phenylmethanesulfonyl fluoride. Equal amounts of protein extracts were separated by using 8% or 10% SDS-PAGE, and then transferred to a polyvinylidene difluoride membrane (Bio-Rad Laboratories Inc). After blocking for 1 hour in a Tris-buffered saline containing 0.1% Tween 20 and 5% BSA, the membrane was probed with various primary antibodies, followed by secondary antibodies conjugated to horseradish peroxidase. The immunoreactivity was revealed by use of a Pierce ECL kit (Thermo Scientific), and the densities of the protein bands were quantified by ImageJ software. Primary antibodies included p-ERK Thr204/205, ERK, p-AKT Ser473, AKT, GAPDH (Cell Signaling Technology).

Pmel-1 adoptive cell transfer in vivo model

C57BL/6 mice were treated with lymphoid-depleting (500cGy) or myeloid-depleting (900cGy) total body irradiation followed by bone marrow transplant and subcutaneous SM1 tumors injection, received 5×10^6 $gp100_{25\text{-}33}$ peptide-activated pmel-1 splenocytes intravenously when tumors reached 3 to 5mm in diameter as previously described (29, 30), and 3 days of daily i.p. administration of 50,000 IU of interleukin2 (IL-2). Activated splenocytes from wild type C57 BL/6 mice were controls. BRAF inhibitor dabrafenib, MEK inhibitor trametinib, vehicle, or combination of dabrafenib and trametinib, were given daily by oral gavage from the day of ACT. Tumors were followed by caliper measurements 3 times per week.

Flow cytometry analysis

SM1 tumors harvested from mice were digested with collagenase (Sigma-Aldrich). Splenocytes and cells obtained from digested SM1 tumors, were stained with antibodies to CD3 BV605 (clone 17A2), Ly6C FITC (Clone AL-21), PD-L1/CD274 PE (Clone MIH5) (Becton Dickinson Biosciences), CD8a BV421 (Clone 53-6.7) (Biolegend), Ly-6G (Gr1) PerCP 5.5 (clone RB6-8C5), CD11b APC (clone M1/70), F4/80 Pacific blue/eFluor450 (clone BM8), CD25 APC (PC61.5), CD4 FITC (RM4-5) (eBioscience), and analyzed with LSR-II or FACSCalibur flow cytometers (Becton Dickinson Biosciences), followed by analysis using Flow-Jo software (FLOWJO, LLC) as previously described (30). Intracellular staining of interferon gamma was done as previously described (30). Intracellular staining of Foxp3 PE (FJK-16s) (eBioscience) was done according to manufacture's recommendations.

In vivo cytotoxicity assay

The assay was conducted as previously described (30). In brief, splenocytes from naive WT C57BL/6 mice were pulsed with 50 mg/mL of $gp100_{25\text{-}33}$ peptide or the same amount of control $OVA_{257\text{-}264}$ peptide. After 1 hour of incubation, $gp100_{25\text{-}33}$-pulsed WT splenocytes were labeled with 6 nmol/L CFSE for 10 minutes at 37C, whereas control $OVA_{257\text{-}264}$-pulsed splenocytes were differentially labeled with a 10-fold dilution of CFSE (0.6 nmol/L). Cells were injected i.v. into experimental mice at 5 days after pmel-1 adoptive cell transfer. After 10 hours, 5 mice per group were sacrificed and their spleens examined for the presence of CFSE-labeled cells. Percent cytotoxic activity was calculated as number of live $gp100_{25\text{-}33}$ pulsed splenocytes divided by the number of live OVA257-264 pulsed splenocytes, which were distinguished on the basis of the 10-fold difference in CSFE fluorescence by flow cytometry.

Bioluminescence imaging

Pmel-1 splenocytes were retrovirally transduced to express firefly luciferase as previously described (29), and used for ACT. Bioluminescence imaging was carried out with a Xenogen IVIS 200 Imaging System (Xenogen/Caliper Life Sciences) as previously described (22, 23).

Microarray data generation and analysis—Total RNAs were extracted using the RNeasy MicroKit (Qiagen) from SM1 tumors. cDNAs were generated, fragmented, biotinylated, and hybridized to the GeneChip Mouse 430 V2 Arrays (Affymetrix). The arrays were washed and stained on a GeneChip Fluidics Station 450 (Affymetrix); scanning was carried out with the GeneChip Scanner 3000 7G; and image analysis with the Affymetrix GeneChip Command Console Scan Control. Microarray analyses were performed in the R statistical programming environment and using Bioconductor suite of packages (41). Expression data were normalized, background-corrected, and summarized using the Robust Multi-Array Average (RMA) algorithm implemented in the R ‘affy’ package (42). Hierarchical clustering was performed using the Euclidean distance as the similarity metric with average linkage clustering. Clustering results were visualized by heat maps generated using the R ‘NMF’ package (43).

Statistical analysis

Descriptive Statistics such as number of observations, mean and standard deviation were reported and presented graphically for quantitative measurements. Normality assumption was checked for outcomes before statistical testing. For measurements such as tumor volume, percentage of tumor infiltrating lymphocytes, quantified imaging data, cytokine expression levels, pairwise comparisons between treatment groups were performed by unpaired t-tests. All hypothesis testing was two-sided and a significance threshold 0.05 for p-value was used. Analyses were carried out using GraphPad Prism (version 6) software (GraphPad Software, La Jolla, CA).

Supplementary Material

Refer to Web version on PubMed Central for supplementary material.

Acknowledgments

We are grateful to Dr. Xiaoyan Wang from UCLA statistical Core for her assistance in statistical analysis. We want to thank Dr. Li Liu, Dr. Tona Gilmer, Dr. Loren Nakamura and Jessica Offord from GSK for their assistance regarding dabrafenib and trametinib. We also want to thank Dr. Nicholas Restifo, Surgery Branch, National Cancer Institute, Bethesda, MD for providing pmel-1 (Thy1.1) transgenic mice and Dr. Robert Prins from UCLA for maintaining the pmel-1 mice.

Funding: Funded by NIH grants P01 CA168585 and P50 CA086306, the Dr. Robert Vigen Memorial Fund, the Ressler Family Foundation, the Wesley Coyle Memorial Fund and the Garcia-Corsini Family Fund (to A.R.). S.H-L. was supported by NIH grant T32 CA09297, ASCO YIA, and Tower Foundation Research Grant. S.M. was supported by UCLA Final Year Dissertation Fellowship (2014-2015). B.H. was supported by the Rio Ortega Scholarship from the Hospital 12 de Octubre, Madrid, Spain. L.R. was supported by the V Foundation-Gil Nickel Family Endowed Fellowship in Melanoma Research and a grant from the Spanish Society of Medical Oncology (SEOM) for Translational Research in Reference Centers. T.G.G. is supported by the NCI/NIH (P01 CA168585, R21 CA169993), an American Cancer Society Research Scholar Award (RSG-12-257-01-TBE), a Melanoma Research Alliance Established Investigator Award (20120279), the National Center for Advancing Translational Sciences UCLA CTSI Grant UL1TR000124, and a Concern Foundation CONquer CanCER Now Award. J.T. is supported by the NIH Ruth L. Kirschstein Institutional National Research Service Award #T32-CA009120. Flow cytometry was performed in the UCLA Jonsson Comprehensive Cancer Center (JCCC) and Center for AIDS Research Flow Cytometry Core Facility that is supported by National Institutes of Health awards CA-16042 and AI-28697, and by the JCCC, the UCLA AIDS Institute, and the David Geffen School of Medicine at UCLA.

References

1. Hodi FS, et al. Improved survival with ipilimumab in patients with metastatic melanoma. The New England journal of medicine. Aug 19.2010 363:711. [PubMed: 20525992]
2. Robert C, et al. Ipilimumab plus dacarbazine for previously untreated metastatic melanoma. The New England journal of medicine. Jun 30.2011 364:2517. [PubMed: 21639810]
3. Topalian SL, et al. Safety, activity, and immune correlates of anti-PD-1 antibody in cancer. The New England journal of medicine. Jun 28.2012 366:2443. [PubMed: 22658127]
4. Brahmer JR, et al. Safety and activity of anti-PD-L1 antibody in patients with advanced cancer. The New England journal of medicine. Jun 28.2012 366:2455. [PubMed: 22658128]
5. Hamid O, et al. Safety and tumor responses with lambrolizumab (anti-PD-1) in melanoma. The New England journal of medicine. Jul 11.2013 369:134. [PubMed: 23724846]
6. Koya RC, et al. BRAF inhibitor vemurafenib improves the antitumor activity of adoptive cell immunotherapy. Cancer research. Aug 15.2012 72:3928. [PubMed: 22693252]
7. Hooijkaas A, et al. Selective BRAF inhibition decreases tumor-resident lymphocyte frequencies in a mouse model of human melanoma. Oncoimmunology. Aug 1.2012 1:609. [PubMed: 22934253]
8. Knight DA, et al. Host immunity contributes to the anti-melanoma activity of BRAF inhibitors. The Journal of clinical investigation. Mar 1.2013 123:1371. [PubMed: 23454771]

9. Cooper ZA, et al. Response to BRAF inhibition in melanoma is enhanced when combined with immune checkpoint blockade. Cancer immunology research. Jul.2014 2:643. [PubMed: 24903021]
10. Boni A, et al. Selective BRAFV600E inhibition enhances T-cell recognition of melanoma without affecting lymphocyte function. Cancer research. Jul 1.2010 70:5213. [PubMed: 20551059]
11. Sapkota B, Hill CE, Pollack BP. Vemurafenib enhances MHC induction in BRAF homozygous melanoma cells. Oncoimmunology. Jan 1.2013 2:e22890. [PubMed: 23483066]
12. Frederick DT, et al. BRAF inhibition is associated with enhanced melanoma antigen expression and a more favorable tumor microenvironment in patients with metastatic melanoma. Clinical cancer research : an official journal of the American Association for Cancer Research. Mar 1.2013 19:1225. [PubMed: 23307859]
13. Donia M, et al. BRAF inhibition improves tumor recognition by the immune system: Potential implications for combinatorial therapies against melanoma involving adoptive T-cell transfer. Oncoimmunology. Dec 1.2012 1:1476. [PubMed: 23264894]
14. Wilmott JS, et al. Selective BRAF inhibitors induce marked T-cell infiltration into human metastatic melanoma. Clinical cancer research : an official journal of the American Association for Cancer Research. Mar 1.2012 18:1386. [PubMed: 22156613]
15. Long GV, et al. Effects of BRAF inhibitors on human melanoma tissue before treatment, early during treatment, and on progression. Pigment cell & melanoma research. Jul.2013 26:499. [PubMed: 23557327]
16. Comin-Anduix B, et al. The oncogenic BRAF kinase inhibitor PLX4032/RG7204 does not affect the viability or function of human lymphocytes across a wide range of concentrations. Clinical cancer research : an official journal of the American Association for Cancer Research. Dec 15.2010 16:6040. [PubMed: 21169256]
17. Ribas A, Hodi FS, Callahan M, Konto C, Wolchok J. Hepatotoxicity with combination of vemurafenib and ipilimumab. The New England journal of medicine. Apr 4.2013 368:1365. [PubMed: 23550685]
18. Su F, et al. RAS mutations in cutaneous squamous-cell carcinomas in patients treated with BRAF inhibitors. The New England journal of medicine. Jan 19.2012 366:207. [PubMed: 22256804]
19. Flaherty KT, et al. Combined BRAF and MEK inhibition in melanoma with BRAF V600 mutations. The New England journal of medicine. Nov.2012 367:1694. [PubMed: 23020132]
20. Hu-Lieskovan S, Robert L, Homet Moreno B, Ribas A. Combining Targeted Therapy With Immunotherapy in BRAF-Mutant Melanoma: Promise and Challenges. Journal of clinical oncology : official journal of the American Society of Clinical Oncology. Jul 20.2014 32:2248. [PubMed: 24958825]
21. Kono M, et al. Role of the mitogen-activated protein kinase signaling pathway in the regulation of human melanocytic antigen expression. Molecular cancer research : MCR. Oct.2006 4:779. [PubMed: 17050671]
22. Vella LJ, et al. MEK inhibition, alone or in combination with BRAF inhibition, affects multiple functions of isolated normal human lymphocytes and dendritic cells. Cancer immunology research. Apr.2014 2:351. [PubMed: 24764582]
23. Overwijk WW, et al. Tumor regression and autoimmunity after reversal of a functionally tolerant state of self-reactive CD8+ T cells. The Journal of experimental medicine. Aug 18.2003 198:569. [PubMed: 12925674]
24. Youn JI, Nagaraj S, Collazo M, Gabrilovich DI. Subsets of myeloid-derived suppressor cells in tumor-bearing mice. Journal of immunology. Oct 15.2008 181:5791.
25. Berchtold S, et al. Cloning, recombinant expression and biochemical characterization of the murine CD83 molecule which is specifically upregulated during dendritic cell maturation. FEBS letters. Nov 19.1999 461:211. [PubMed: 10567699]
26. Chen C, Gault A, Shen L, Nabavi N. Molecular cloning and expression of early T cell costimulatory molecule-1 and its characterization as B7-2 molecule. Journal of immunology. May 15.1994 152:4929.
27. Liu C, et al. BRAF inhibition increases tumor infiltration by T cells and enhances the antitumor activity of adoptive immunotherapy in mice. Clinical cancer research : an official journal of the American Association for Cancer Research. Jan 15.2013 19:393. [PubMed: 23204132]

28. Sumimoto H, Imabayashi F, Iwata T, Kawakami Y. The BRAF-MAPK signaling pathway is essential for cancer-immune evasion in human melanoma cells. The Journal of experimental medicine. Jul 10.2006 203:1651. [PubMed: 16801397]
29. Wang J, et al. B7-H3 associated with tumor progression and epigenetic regulatory activity in cutaneous melanoma. The Journal of investigative dermatology. Aug.2013 133:2050. [PubMed: 23474948]
30. Jiang X, Zhou J, Giobbie-Hurder A, Wargo J, Hodi FS. The activation of MAPK in melanoma cells resistant to BRAF inhibition promotes PD-L1 expression that is reversible by MEK and PI3K inhibition. Clinical cancer research : an official journal of the American Association for Cancer Research. Feb 1.2013 19:598. [PubMed: 23095323]
31. Cooper ZA, Frederick DT, Ahmed Z, Wargo JA. Combining checkpoint inhibitors and BRAF-targeted agents against metastatic melanoma. Oncoimmunology. May 1.2013 2:e24320. [PubMed: 23762807]
32. Gabrilovich DI, Nagaraj S. Myeloid-derived suppressor cells as regulators of the immune system. Nature reviews. Immunology. Mar.2009 9:162.
33. Daud AI, et al. Phenotypic and functional analysis of dendritic cells and clinical outcome in patients with high-risk melanoma treated with adjuvant granulocyte macrophage colony-stimulating factor. Journal of clinical oncology : official journal of the American Society of Clinical Oncology. Jul 1.2008 26:3235. [PubMed: 18591558]
34. Diaz-Montero CM, et al. Increased circulating myeloid-derived suppressor cells correlate with clinical cancer stage, metastatic tumor burden, and doxorubicin-cyclophosphamide chemotherapy. Cancer immunology, immunotherapy : CII. Jan.2009 58:49. [PubMed: 18446337]
35. Porembka MR, et al. Pancreatic adenocarcinoma induces bone marrow mobilization of myeloid-derived suppressor cells which promote primary tumor growth. Cancer immunology, immunotherapy : CII. Sep.2012 61:1373. [PubMed: 22215137]
36. Wang L, et al. Increased myeloid-derived suppressor cells in gastric cancer correlate with cancer stage and plasma S100A8/A9 proinflammatory proteins. Journal of immunology. Jan 15.2013 190:794.
37. Yuan XK, Zhao XK, Xia YC, Zhu X, Xiao P. Increased circulating immunosuppressive CD14(+)HLA-DR(−/low) cells correlate with clinical cancer stage and pathological grade in patients with bladder carcinoma. The Journal of international medical research. 2011; 39:1381. [PubMed: 21986138]
38. Fife BT, Pauken KE. The role of the PD-1 pathway in autoimmunity and peripheral tolerance. Annals of the New York Academy of Sciences. Jan.2011 1217:45. [PubMed: 21276005]
39. Dong H, et al. Tumor-associated B7-H1 promotes T-cell apoptosis: a potential mechanism of immune evasion. Nature medicine. Aug.2002 8:793.
40. Iwai Y, et al. Involvement of PD-L1 on tumor cells in the escape from host immune system and tumor immunotherapy by PD-L1 blockade. Proceedings of the National Academy of Sciences of the United States of America. Sep 17.2002 99:12293. [PubMed: 12218188]
41. Gentleman RC, et al. Bioconductor: open software development for computational biology and bioinformatics. Genome biology. 2004; 5:R80. [PubMed: 15461798]
42. Gautier L, Cope L, Bolstad BM, Irizarry RA. affy--analysis of Affymetrix GeneChip data at the probe level. Bioinformatics. Feb 12.2004 20:307. [PubMed: 14960456]
43. Gaujoux R, Seoighe C. A flexible R package for nonnegative matrix factorization. BMC bioinformatics. 2010; 11:367. [PubMed: 20598126]

One Sentence Summary

MEK inhibition enhanced the antitumor activity of combined BRAF inhibition and immunotherapy.

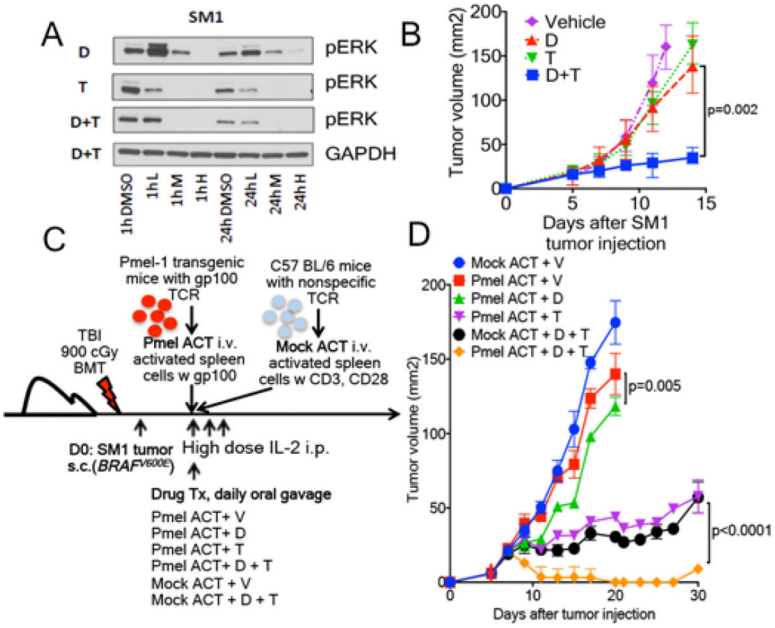

Fig. 1. Enhanced *in vivo* antitumor activity with pmel-1 adoptive cell transfer (ACT) plus dabrafenib (D) and/or trametinib (T)

(A) Western blot analysis of MAPK pathway. SM1 cells were treated with serial dilutions of D, T, or D+T for 1 and 24 hours. L: low dose (D 0.1μM/T 0.005μM). M: medium dose (D 5μM/T 0.25μM). H: high dose (D 20μM/T 1μM). **(B)** *In vivo* tumour growth curves with 4 mice in each group (mean+/−SD). SM1 bearing C57BL/6 mice were treated with D 30mg/kg, T 0.15mg/kg, or the combination via oral gavage daily, started when tumours were 3-5mm. **(C)** Schema of pmel-1 ACT model. C57BL/6 mice had myeloid-depleting total body irradiation (TBI) followed by bone marrow transplant (BMT) and SM1 tumour injections. When tumours reached 3mm, three million $gp100_{25\text{-}33}$ peptide activated pmel-1 splenocytes (pmel-1 transgenic mice carrying T cell receptor specific for melanoma antigen gp100) were injected. Wild type C57 BL/6 mouse splenocytes activated by CD3 and CD28 were mock ACT controls. Both ACT were followed by high dose IL-2 for 3 days. Daily oral gavage of vehicle control (V), D 30mg/kg, T 0.6mg/kg, or the combination were started on the day of ACT. **(D)** *In vivo* SM1 tumour growth curves with 3-4 mice in each group (mean +/−SD), after D, T and ACT treatments. $P < 0.0001$ by unpaired t test on day 30, pmel-1 ACT+D+T vs pmel-1 ACT +T, or vs mock ACT +D+T.

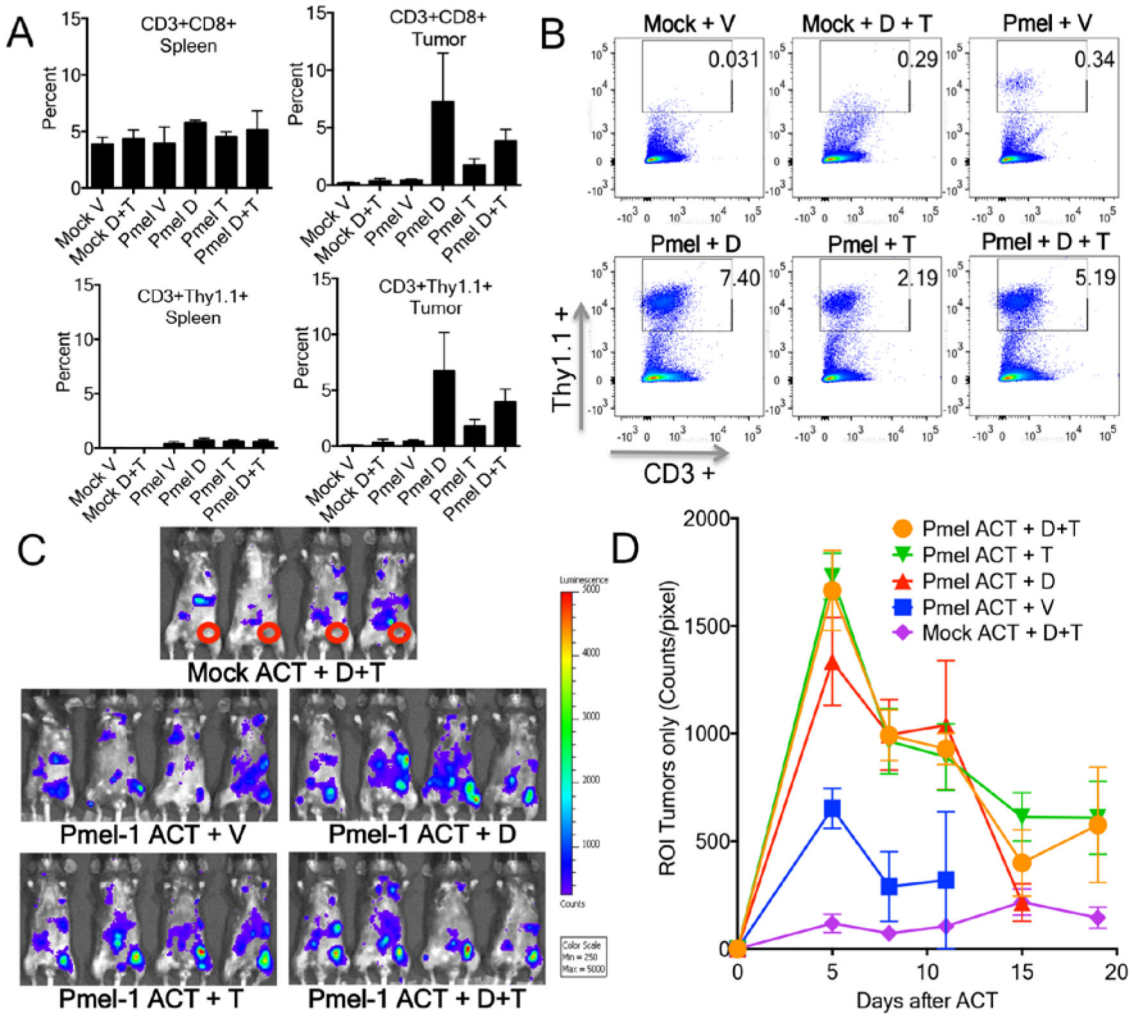

Fig. 2. Increased tumor infiltrating lymphocytes (TILs) with pmel-1 ACT plus dabrafenib and/or trametinib in SM1 tumors

(A) Quantification of TILs. Splenocytes and TILs harvested on day 5 after ACT were counted and analysed by flow cytometry for Thy1.1/CD3/CD8 staining (3 mice in each group, mean+/−SD). Percentage of effectors (CD3+CD8+ or CD3+Thy1.1+) were shown to be statistically significantly changed by unpaired t test in several subgroups (CD3+CD8+ TILs: p=0.049 pmel D vs pmel V, p=0.02 pmel T vs pmel V, p=0.004 pmel D+T vs pmel V, p=0.035 pmel D+T vs pmel T; CD3+Thy1.1+: p=0.03 pmel D vs pmel V, p=0.02 pmel T vs pmel V, p=0.006 pmel D+T vs pmel V, p=0.047 pmel D+T vs pmel T). **(B)** Representative flow data of percentage of CD3+Thy1.1+ TILs is shown. **(C)** *In vivo* bioluminescent imaging (BLI) of adoptively transferred lymphocytes. Pmel-1 transgenic T cells were transduced with a retrovirus-firefly luciferase and used for ACT. Representative figure on day 5 depict 4 replicate mice per group. **(D)** Quantification of BLI of serial images with region of interest (ROI) analysis at the site of tumours (counts/pixel) obtained through day 18 post-ACT of luciferase expressing pmel-1 T-cells (4 mice per group, mean+/−SD). On Day 5, p=0.0009 pmel D vs pmel V, p<0.0001 pmel T vs pmel V, p<0.0001 pmel D+T vs pmel V, p=0.01 pmel T or pmel D+T vs pmel D (unpaired t test, n=4).

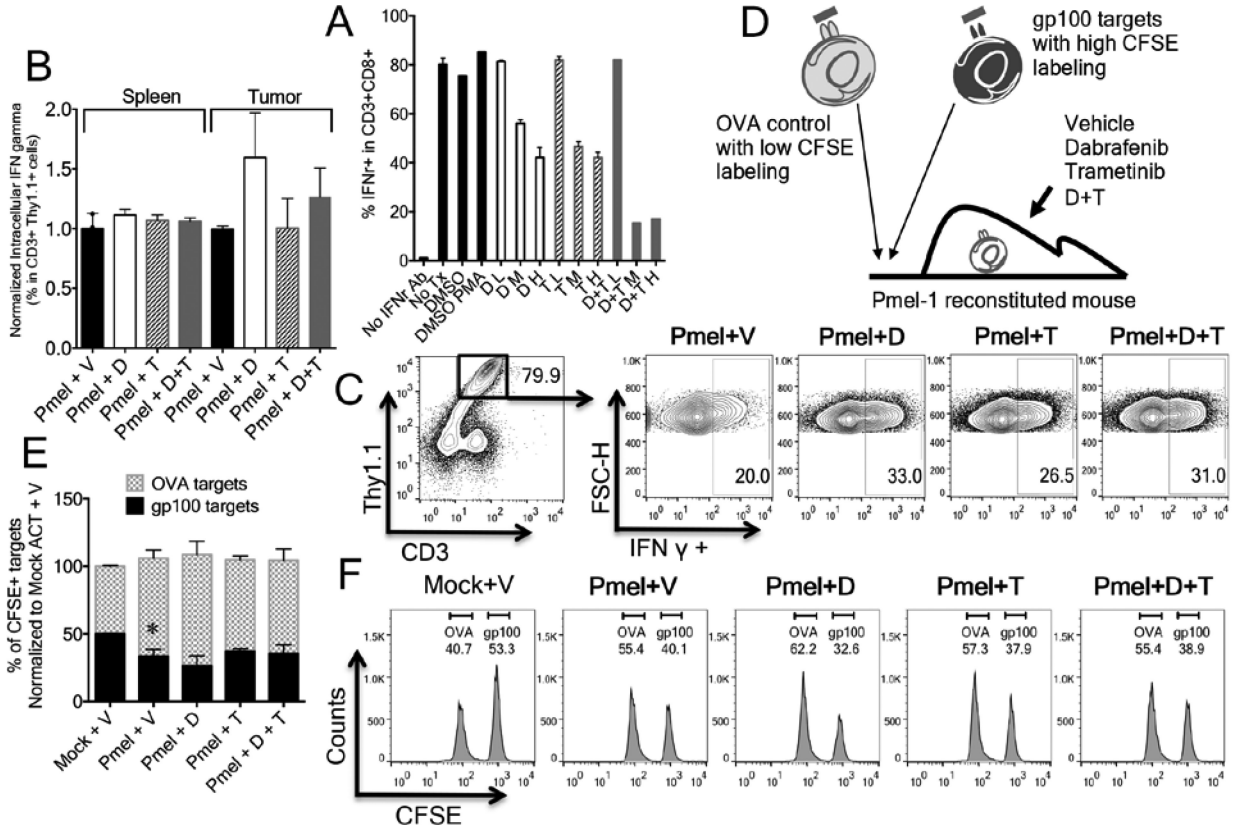

Fig. 3. Dabrafenib, trametinib or combination impairs effector T cell function *in vitro* but not *in vivo*

(A) *In vitro* study of cytokine-producing function of effector cells. $Gp100_{25\text{-}33}$-activated pmel-1 mouse splenocytes were treated at serial dilutions of D, T, or D+T for 72 hours. L: low dose (D 0.1μM/T 0.005μM). M: medium dose (D 5μM/T 0.25μM). H: high dose (D 20μM/T 1μM). Cells were analysed by FACS for CD3/CD8/IFN-γ staining. Bar graph of percentage of IFN-γ expressing CD3+ CD8+ cells are shown (mean+/−SD). p=0.002 DM or DH vs DL, p=0.045 DH vs DM, p=0.003 TM or TH vs TL, p=0.0002 D+T M or D+T H vs D+T L (unpaired t test, n=3). **(B)** *In vivo* effect on cytokine production upon antigen re-stimulation. SM1 tumour-bearing C57BL/6 mice received pmel-1 ACT with or without D and T. On day 5 post-ACT, spleens and TILs were isolated for intracellular IFN-γ staining analysed by FACS after 5-hour *ex vivo* exposure to the $gp100_{25\text{-}33}$ peptide. Percentage of IFN-γ expressing CD3+Thy1.1 cells in the spleen and tumor was normalized to Pmel + V (mean+/−SD). **(C)** Gating strategy and representative flow data is shown. **(D)** Schema of the *in vivo* cytotoxic T cell assay. C57BL/6 mice received ACT of 5×10^4 pmel-1 splenocytes and daily D, T, D+T or vehicle via oral gavage. On day 5, mice received an intravenous challenge with CFSE-labelled target cells (splenocytes pulsed with $gp100_{25\text{-}33}$ peptide or control OVA peptide). $Gp100_{25\text{-}33}$ pulsed targets were pulsed with 10 times more concentrated of CFSE than OVA pulsed cells. Ten hours later, splenocytes were harvested and analysed by FACS. **(E)** Bar graph representation of the in vivo cytotoxicity study result (mean+/−SD). p=0.01 pmel V vs mock V (34% down, unpaired t test, n=3). (F). Representative flow data is shown.

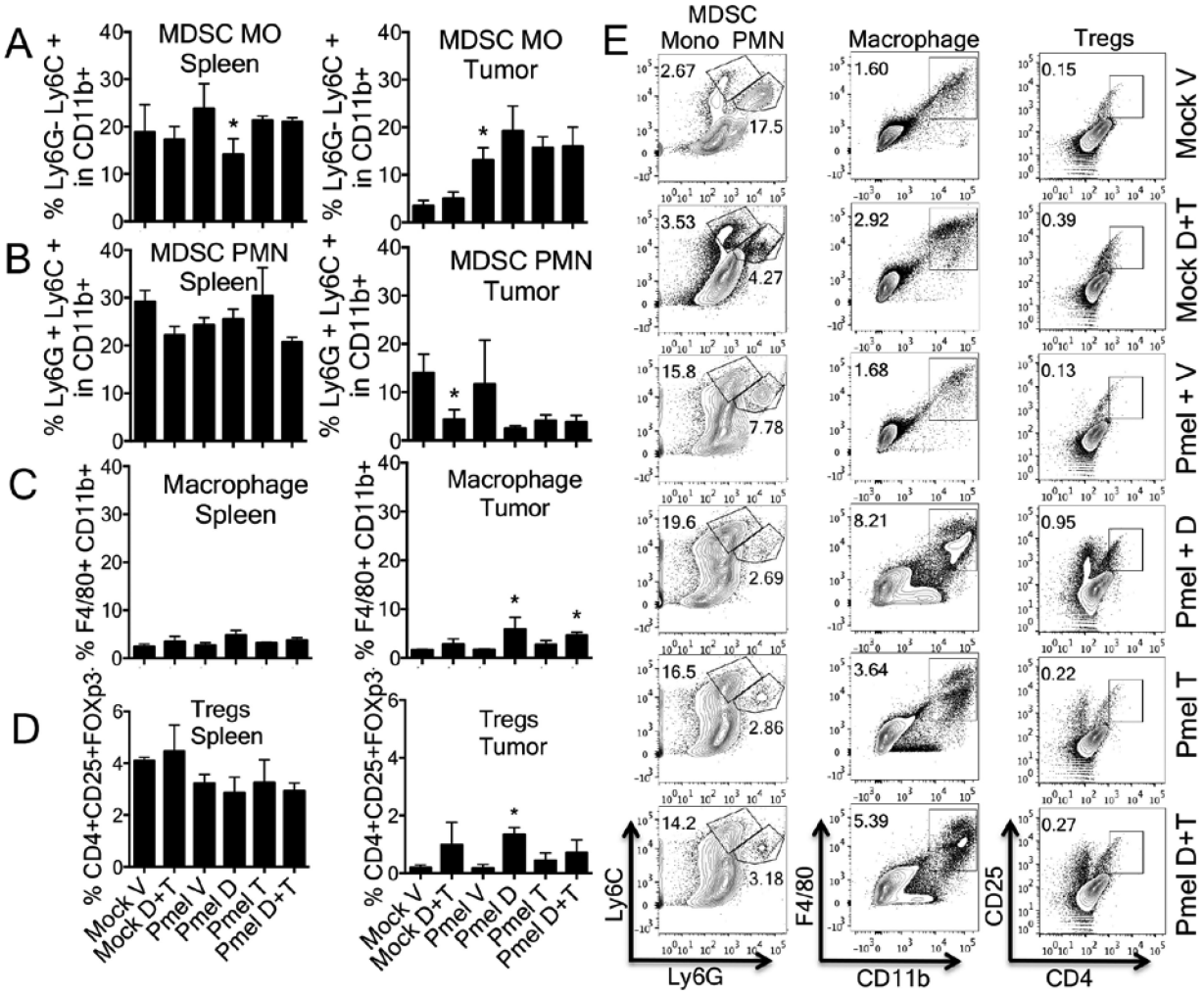

Fig. 4. Dabrafenib and trametinib changed the cellular components of the tumour microenvironment

On day 5 post-ACT, spleens and tumours were isolated and stained with fluorescent-labelled antibodies, analysed by FACS with 3 mice in each group (mean+/−SD). **(A)** MO-MDSC (CD11b+Ly6C^{Hi} Ly6G^{Lo}) presented as percentage of CD11b+ cells. * p=0.06 pmel D vs pmel V in spleen, p=0.009 pmel V vs Mock V in tumor (unpaired t test, n=3). **(B)** PMNMDSC (CD11b+Ly6C^{Low}Ly6G^{Hi}) presented as percentage of CD11b+ cells. * p=0.002 mock D+T vs mock V in tumor (unpaired t test, n=3). **(C)** Analysis of macrophages (F4/80+CD11b+). * p=0.04 pmel D vs pmel V, p=0.002 pmel D+T vs pmel V, both in tumors (unpaired t test, n=3). **(D)** Analysis of T regulatory cells (Tregs, CD4+CD25+FOXp3+). * P=0.002 pmel D vs pmel V in tumors (unpaired t test, n=3). **(E)** Gating strategy and representative FACS plots in tumours.

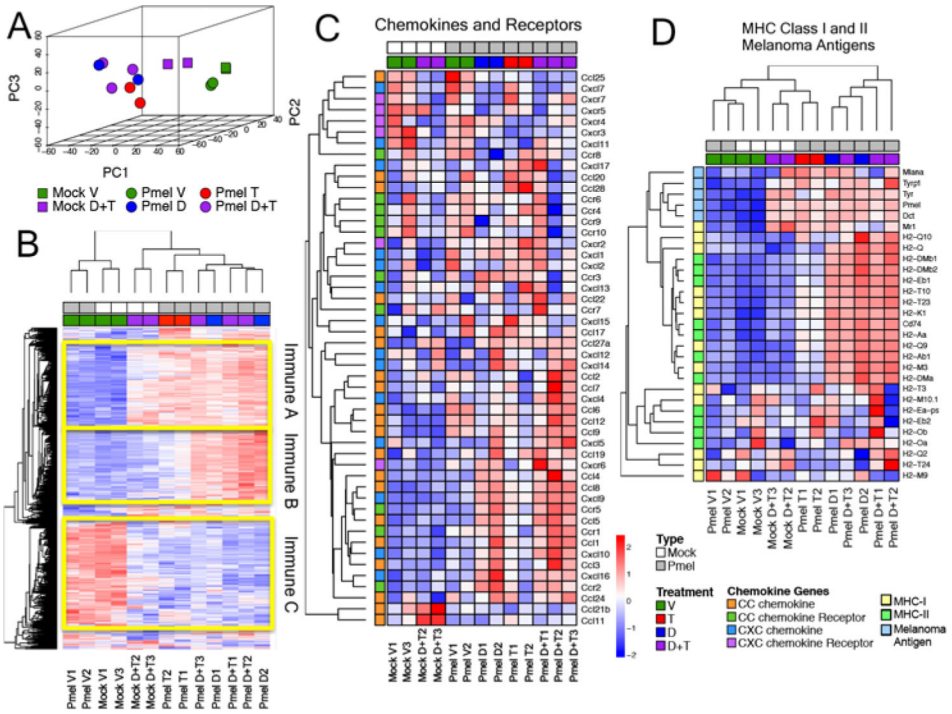

Fig. 5. Microarray analysis of tumors treated by dabrafenib, trametinib, or combination of dabrafenib and trametinib combined with pmel-1 ACT or mock ACT

On day 5 post-ACT, tumours were isolated and snap frozen immediately (two to three mice in each group). RNA isolation was done after all samples were collected. **(A)** Principal component analysis of gene expression profile of the tested samples. **(B)** Clustering of immune-related genes with ANOVA filter $p<0.05$. Gene names in individual clusters are listed in supplemental tables 1-3. **(C)** Clustering of chemokines and their receptors. **(D)** Clustering of MDAs and MHC class I and II molecules.

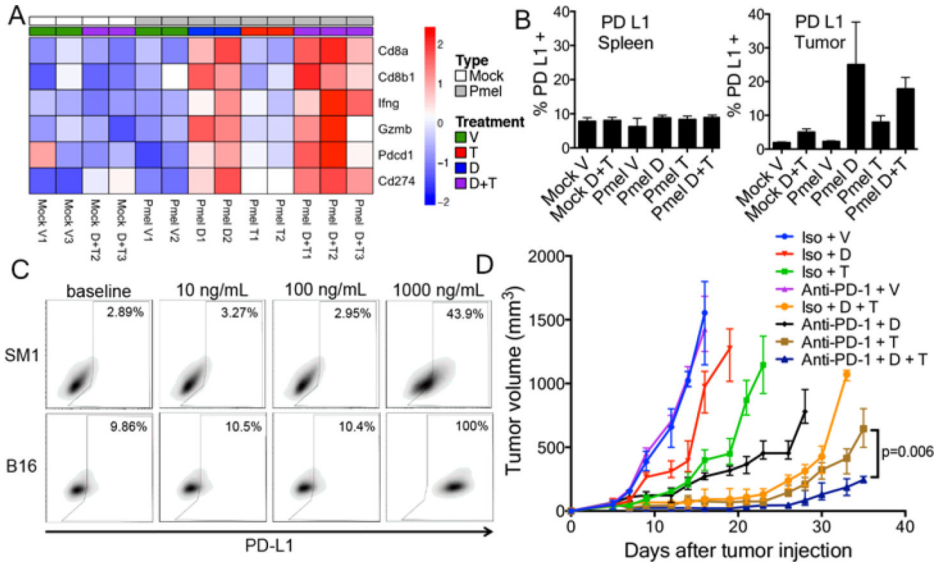

Fig. 6. Up-regulation of PD-L1 and triple combination of dabrafenib, trametinib with PD-1 blockade is superior in antitumor effect against SM1

(A) Heat map representation of CD8, granzyme B, IFNγ, PD-1, PD-L1 gene expression from microarray data (PD-L1: p=0.01 mock D+T vs mock V, p=0.004 pmel T vs pmel V, p=0.004 pmel D+T vs pmel V, p=0.03 pmel T vs pmel D+T, unpaired t test, n=3). **(B)** Percentage of PD-L1-expressing cells in the spleen and tumours 5 days after ACT and drug treatments started, 3 mice in each group (mean+/−SD). P=0.006 mock D+T vs mock V, p=0.04 pmel D vs pmel V, p=0.007 pmel T vs pmel V, p=0.001 pmel D+T vs pmel V. **(C)** Expression of PD-L1 on SM1 after 18 hours of IFNγ stimulation at different concentrations. B16 cells served as positive control. **(D)** *In vivo* SM1 tumour growth curves after D, T and anti-PD1 treatments, 4 mice in each group (mean+/−SD). SM1 tumour bearing C57 BL/6 mice received anti-PD1 (Merck DX400) 200μg via intraperitoneal injection every 4 days, started when tumours reaches 3-5mm. Daily oral gavage of vehicle control (V), D 30mg/kg, T 0.6mg/kg, or the combination were started on the same day as anti-PD1.